EUROPEAN ORGANIZATION FOR NUCLEAR RESEARCH

Proposal to the ISOLDE and Neutron Time-of-Flight Committee

Single-particle aspects of high-J *sd-fp* shell mirror energy differences (MEDs)

September 25, 2023

C. R. Hoffman[1], S. J. Freeman[2,3], D. K. Sharp[2], L. Gaffney[4], Y. Ayyad[5], M. A. Bentley[6], K. Bhatt[1], P. Bulter[4], J. Chen[7], B. P. Kay[1], A. N. Kuchera[8], M. Labiche[9], I. Lazarus[9], S. M. Lenzi[10,11], R. Lubna[12], P. T. MacGregor[3], R. Page[4], R. Raabe[13], F. Recchia[10,14], K. Rezynkina[11], N. Sensharma[1], and T. L. Tang[15]

[1]*Physics Division, Argonne National Laboratory, Argonne, IL 60439, USA*
[2]*Schuster Laboratory, The University of Manchester, Oxford Road, Manchester M13 9PL, UK*
[3]*ISOLDE, CERN, CH-1211 Geneva 23, Switzerland*
[4]*Oliver Lodge Laboratory, University of Liverpool, Liverpool, L69 7ZE, UK*
[5]*IGFAE, Universidade de Santiago de Compostela, E-15782, Santiago de Compostela, Spain*
[6]*Department of Physics, University of York, Heslington, York YO10 5DD, United Kingdom*
[7]*College of Science, Southern University of Science and Technology, Shenzhen, 518055, Guangdong, China* [8]*Department of Physics, Davidson College, Davidson, NC 28035, USA*
[9]*STFC Daresbury Laboratory, Daresbury, Warrington, WA4 4AD, UK*
[10]*Dipartimento di Fisica e Astronomia, Università degli Studi di Padova*
[11]*INFN, Sezione di Padova, I-35131 Padova, Italy*
[12]*FRIB, Michigan State University, East Lansing, MI 48824, USA*
[13]*KU Leuven, Institut voor Kern- en Stralingsfysica, 3001 Leuven, Belgium*
[14]*INFN, Laboratori Nazionali di Legnaro, I-35020 Legnaro, Italy*
[15]*Department of Physics, Florida State University, Tallahassee, FL 32306, USA*

CERN-INTC-2023-054 / INTC-P-670
25/09/2023

Co-Spokespersons: S. J. Freeman [sean.freeman@cern.ch]
C. R. Hoffman [crhoffman@anl.gov]
Contact person: P. T. MacGregor [patrick.macgregor@cern.ch]

Abstract: A proposal is made to determine the single-neutron adding strengths in ^{39}K via the ^{38}K(d,p) reaction. The focus is on the negative parity high-spin states, through the terminating J^{π}=13/2^{-} level, which make up one side of the $T = 1/2$ $A = 39$ mirror energy differences (MEDs). Extraction of the neutron strength as a function of spin will provide a unique perspective on the evolution of the MEDs between the ^{39}K-^{39}Ca pair. Specifically, new insight will be gained as to whether changes in the makeup of the wave

functions, for instance an increase in one single-particle configuration over others, are the root of the increase in the MEDs observed at higher J. The proposed work will provide the first direct data on the single-particle aspects of these levels involved in the MEDs. The measurement will utilize the established techniques for single-neutron adding (d,p) transfer at the ISOLDE Solenoid Spectrometer (ISS) and a ^{38}K beam provided by HIE-ISOLDE at 7.5 MeV/u. A total of **9** shifts of beam time is requested.

Requested shifts: [9] total shifts over a single time-frame, no split.

Motivation

Mirror energy differences (MEDs) between analog excited states, when viewed as a function of total angular momentum J as MED(J) =E$_x(J, T_z = +1/2) - E_x(J, T_z = -1/2)$, provide isospin-symmetry tests along the collectivity plane. Additional insight into the nature of the wave functions and the extent of the radii of the levels involved is also possible by leveraging information from large-scale shell-model calculations (see Refs. [1, 2, 3, 4, 5, 6] and those within). For nuclei with active orbitals in the $1s0d-0f1p$ shell regions, MEDs have been determined up to and beyond pairs of levels consisting of fully-aligned configurations. The $T = 1/2$, $A = 39$ MEDs of ^{39}K and ^{39}Ca, which are central to the proposed work, have been determined up through $J^\pi = 19/2^-$ as shown in Fig. 1 [7]. Likewise, high-J MEDs for the $A = 35$ pair [8, 9] (^{35}Cl-^{35}Ar) as well as for the $A = 31$ pair [10, 11, 12] (^{31}S-^{31}P) have also been observed.

These three sets of nuclei are structurally linked, each having an odd-N, odd-Z core contained within the *sd* shell. Naturally, their MEDs track in a similar pattern as a function of spin for both positive- and negative- parity states. In all cases, the positive-parity states, expected to be dominated by *sd*-shell configurations, give MEDs that are smooth and reside below $\approx 50 - 100$ keV. However, for the negative-parity fp-shell intruder levels, larger MEDs of > -200 keV have been observed at larger J. These are shown in the top row of Fig. 2 for the $A = 35$ and 39 cases. The abrupt change in the MEDs have been thought to occur due to increased purity in their single-nucleon configurations for one, or both, of the mirror states involved. However, **no experimental information exists on the single-particle content of the involved levels.** The negative-parity levels are anticipated to be primarily built upon a neutron residing within the $0f_{7/2}$ orbital and the largest MEDs have been observed for $J^\pi \geq 13/2^-$. Occupancy of the $\nu 1p_{3/2}$ orbital is also allowed at lower spin though only expected to contribute significantly at high excitation energy due to the $N = 28$ gap surviving in this region. It is worth mentioning that the MEDs of the non-yrast $11/2^-_2$ levels in the $A = 35$ and 39 systems are also larger than those of the lower J MEDs.

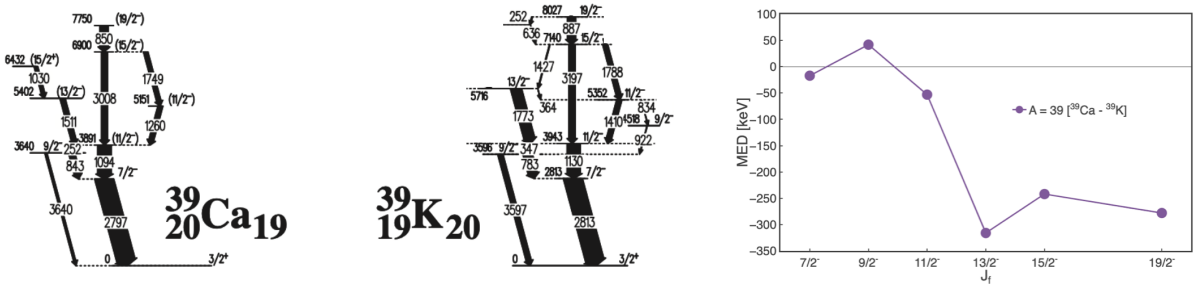

Figure 1: Partial high-spin level schemes of the T_z=±1/2 A=39 mirror nuclei ^{39}Ca and ^{39}K (adopted from Ref. [7]) and the corresponding mirror energy differences (MEDs) between the yrast $\pi = -$ fp-shell intruder levels.

The origin of the larger MEDs observed for the higher-J levels has been discussed in terms of differences in the radii between the mirror levels and as a consequence of changes in their underlying single-particle configurations [1, 2, 3, 7, 9, 10, 12]. For instance, it is possible that a single-particle configuration, either proton *or* neutron, grows to dominate the wave function at higher spin due to limitations in the configuration space. These levels are in contrast to pairs of states where each have a balanced contribution from both proton *and* neutron excitations. Hence, in the latter case the levels would present similar radial sizes and more cohesive overlap. In our present case, and similarly for the $A = 35$ case, the expectation is that as the cross-shell excitations (from within the *sd*-shell into the fp-shell in this case) push towards higher-J, they do in fact become increasingly dominated by a lone single-particle configuration (either pure proton or pure neutron). The pinnacle of this concept is when the formation of the aligned state is reached at maximum possible spin, $J_{max} = 13/2^-$, where only the $(0d_{3/2})^2_{J=3}(0f_{7/2})^1_{J=7/2}$ configuration is possible. These arguments are certainly in line with the observed jump in the MEDs from the yrast $11/2^-$ state to the yrast $13/2^-$ state for the $A = 35$ and 39 cases (top row of Fig. 2).

Single-neutron overlap values, (C^2S), determined from shell-model calculations that were performed with the FSU cross-shell interaction [13], were investigated to quantify the simple scenario presented above. The $0f_{7/2}$ $\ell = 3$ single-neutron overlaps between the initial $J = 3^+$ levels in both ^{34m}Cl and ^{38}K with the final negative parity yrast levels in ^{35}Cl and ^{39}K, respectively, are shown on the bottom row of Fig. 2. The proposed determination of the ^{38}K(d,p) data will provide the proper values in which to compare with these calculations. An independent measurement to determine the values from the ^{34m}Cl(d,p) reaction has also been approved for beam time using the HELIOS spectrometer located at the ATLAS Facility, Argonne, USA. As shown in the bottom row of Fig. 2 the C^2S values for both mass sets follow a similar trend increasing in strength between $J = 11/2^-$ and $13/2^-$. This increase in the single-neutron component follows directly with the simple picture laid out above. Subtle differences do exist between the $A = 35$ and $A = 39$ cases, however, where the latter shows an increase in the fragmentation or strength at lower J. It is possible that the additional nucleons residing within the $0d_{3/2}$ orbital for the $A = 39$ systems contribute to larger core-coupling effects. The

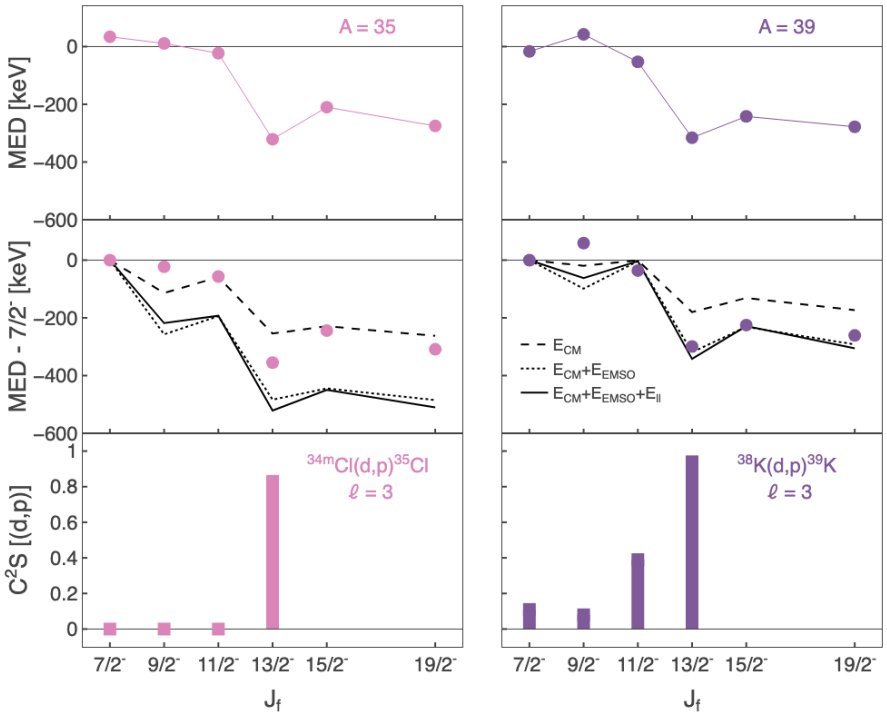

Figure 2: (top row) The measured Mirror Energy Differences (MEDs) for the yrast negative parity states in the A=35 (left) and A=39 (right) T=1/2 mirror systems. (middle row) The data of the top row relative to the $7/2^-$ value and with the inclusion of the calculated MEDs as adopted from Ref. [9]. The contribution from each component to the MEDs is indicated by the different line types and noted in the caption (see text for details). (bottom row) The calculated single-neutron overlaps (C^2S values in Table 1) between the 3^+ level in the initial T=0 nucleus and the final $\pi = -$ levels in the $N+1$ systems. The C^2S values are for $\ell = 3$ transfer based on the FSU cross-shell effective interaction [13] (note that no $\ell = 1$ strength was predicted to any of these yrast levels).

complementary data to be collected in the proposed $A = 39$ work and in the planned work at ATLAS for the $A = 35$ case [14] will be of great interest to these topics.

To further quantify the importance of the single-particle configurations on the present understanding of the aforementioned MEDs, a deconstructed view of theoretical calculations for the $A = 35$ and 39 mirrors relative to their $7/2^-$ MED value are shown along the middle row of Fig. 2 (as adopted from Fig. 4 of Ref. [9] and Figs. 30 and 31 of Ref. [3]). Similar information is also shown in Fig. 5 of Ref. [15] for the $A = 31$ MEDs. The three terms of the theoretical calculation include the multipole Coulomb term (E_{CM}), the electromagnetic spin-orbit coupling (E_{EMSO}) and an orbital momentum coupling term ($E_{\ell\ell}$). The E_{EMSO} and $E_{\ell\ell}$ terms highlight single-particle contributions to the MEDs as they are proportional to occupancy differences (radii) between neutron and proton orbitals in the neutron-rich versus proton-rich nucleus, respectively. Of these two, the E_{EMSO} term is largest. This is not surprising as the term is enhanced between nucleons in orbits of opposite spin projections, in this case the $0d_{3/2}$ and $0f_{7/2}$ orbitals . The total sum of all

components show good agreement with the trends in both of the MED sets and reproduce nearly all of the $A = 39$ data. In the $A = 35$ case, it is possible the lack of a quantitative reproduction is due to a lack of inclusion of the lower $0d_{5/2}$ orbital, and hence, the additional correlations associated with the larger valence space. The comparison of the neutron-strengths between the $A = 35$ and 39 systems will also shed light on this point.

Table 1: The excitation energies and calculated single-neutron adding overlaps (C^2S) from the $J = 3^+$ states in ^{34m}Cl and ^{38}K to their corresponding yrast negative parity states (and $11/2^-_2$ states) in the $N + 1$ systems. The overlaps were calculated using the FSU cross-shell effective interaction [13]. Total count estimates were made incorporating an experimental acceptance of 60%, the C^2S values plus a quenching factor of 0.6, a beam rate of 2×10^6 pps, a CD_2 target thickness of 100 μg/cm^2 and cross sections calculated by the DWBA prescription.

			^{34m}Cl		^{38}K			
J_i	J_f	ℓ	Ex	C^2S	Ex	C^2S	σ [mb]	Tot. Counts [8 shfits]
	$7/2^-$	3	3.163	< 0.1	2.814	0.11	0.78	98
	$9/2^-$	3	4.348	< 0.1	3.596	0.08	1.08	99
3^+	$11/2^-$	3	5.407	< 0.1	3.943	0.39	1.36	607
	$13/2^-$	3	6.087	0.83	5.716	0.94	2.08	2238
	$11/2^-_2$	3	5.927	0.22	5.353	0.47	1.68	904

Focus of the Measurement

The goal of the proposed measurement is to **extract the relative single-neutron overlaps between the ^{38}K $J = 3^+$ ground state and the known yrast $7/2^-$ (2.814 MeV), $9/2^-$ (3.596 MeV), $11/2^-$ (3.943 MeV), and $13/2^-$ (5.716 MeV) states, as well as the known non-yrast $11/2^-$ state (5.353 MeV), in ^{39}K.** The appropriate single-neutron adding reaction at the appropriate energy, ^{38}K(d,p)^{39}K at 7.5 MeV/u, will be used. The access to higher-J states is made possible via $\ell = 3$ transfer onto the ^{38}K $J = 3^+$ ground state. This will be the first quantitative test of the single-neutron nature of such high-J states in this $A = 39$ system. The data will provide a sensitive test of the expected wave functions of these levels and quantitatively inform the calculated E_{EMSO} and $E_{\ell\ell}$ single-particle contributions to the large relative MEDs appearing in these nuclei. In addition, the $A = 39$ data will complement an approved measurement to determine the same properties in the $A = 35$ system, ^{35}Cl [14], further testing the description of the wave functions of these levels.

Experimental details

The ^{38}K(d,p) reaction at 7.5 MeV/u on the $J^\pi = 3^+$ ground state will provide access to negative parity states up through $13/2^-$ via $\ell = 3$ neutron transfer (and the $3/2^-$ - $9/2^-$ levels via $\ell = 1$ or $\ell = 3$). Only the ^{39}K $3/2^+$ ground state will be populated via $\ell = 2$

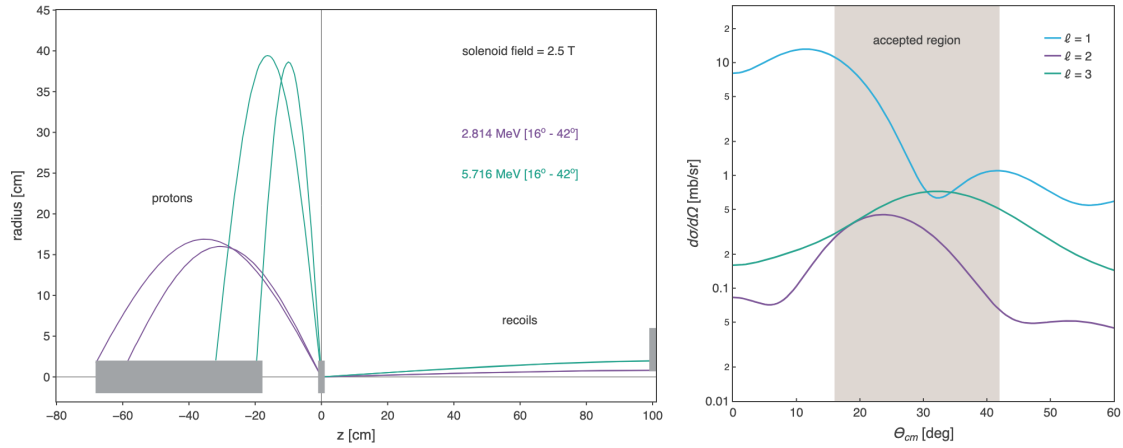

Figure 3: (left) A schematic of the experimental setup and the reaction kinematics for levels at 2.5 and 6.0 MeV in ^{39}K and for each of their minimum and maximum covered center of mass angles, 16° and 42°. The grey boxes represent the Si array coverage, the CD_2 target position and the Si recoil telescope positions moving from left to right, respectively. (right) Calculated angular distributions based on the DWBA prescription using the global optical model parameters of Refs. [16, 17] for three different neutron orbital angular momentum (ℓ) transfer values to indicate their distinct shapes. The grey band indicates the approximate accepted angular range for the states of interest and the proposed experimental setup.

transfer with any sizeable amount in terms of the positive-parity states. The reaction energy provides both excellent momentum matching for the $\ell = 3$ neutron transfer as well as distinguishable angular distributions between other possible ℓ values, most notably $\ell = 1$ (see Fig. 3). The experimental setup has been designed to ensure the acceptance of excited levels between the yrast $7/2^-$ and the yrast $13/2^-$ state (∼2.5-6.0 MeV). The setup also provides center-of-mass angular coverage of ∼16° - 40° for these states covering the peak of the $\ell = 3$ distribution and more. It should be noted that a similar measurement of the ^{38}K(d,p) reaction has taken place at the ReA Facility at FRIB. The experiment utilized the ORRUBA array and was done at a lower beam energy and with a composite ground state / isomer beam [18]. In that work, in addition to the extra complications provided by the composite beam, the focus of the reaction was on low-momentum transfer to states of astrophysical importance and was not optimized for the higher $\ell = 3$ neutron transfer as is the case in the present work.

Beam

The ^{38}K beam of interest is listed at rates of 1.8×10^8 Yield/μC in the yield database which gives an estimated lower limit on the rate of 2×10^6 pps for an energy of 7.5 MeV/u at the ISS. Under our preference for the use of the Ti rod target, the isomer content in the ^{38}K beam is ×100 below the ground state. Similarly, contamination from isobars, ^{38}Ar in particular, are able to be suppressed using a surface ion source, though if present are also able to be distinguished by the Si recoil detectors. Whilst the preference is to use the Ti rod target, if a Ti foil target is utilized in place of the rod, the isomer fraction is expected to be different and so a measurement of the isomer fraction will take place to deduce its

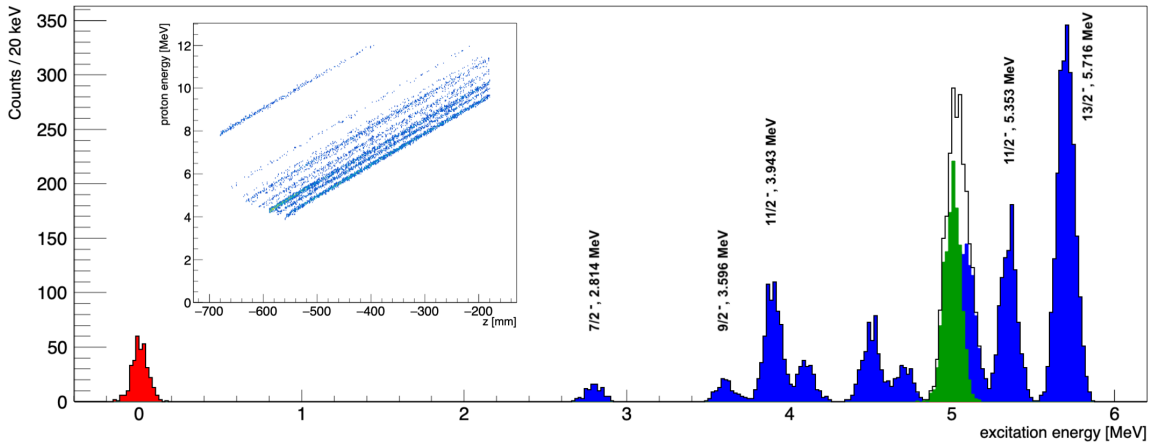

Figure 4: A simulated excitation energy spectrum of the ^{39}K levels populated in via the proposed ^{38}K(d,p) reaction. Levels up to 6 MeV in excitation, all of which are known experimentally, were included with the expected resolution of 125 keV FWHM. The relative peak intensities include the calculated spectroscopic overlaps (C^2S values in Table 1), the relative cross sections and distributions from the DWBA calculations ($\ell = 1$ in green, $\ell = 2$ in red, and $\ell = 3$ in blue) as well as the experimental setup constraints. The total counts reflect those estimated in the last column of Table 1. The inset shows the positioning of the levels in proton energy vs. distance from the target.

level.

The experimental setup

The experimental setup of the ISS will match those used previously to carry out (d,p) reactions in this mass region such as the successful ^{27}Na(d,p) and ^{49}Ca(d,p) experiments. The ISS Si array will be located upstream of a 100 μg/cm^2 CD_2 target ($z = 0$ mm) ranging from from -680 mm $< z < -180$ mm. This arrangement accept protons from θ_{cm} $\sim$16°-42° for the states in ^{39}K ranging from $\sim$2.5-6 MeV in excitation energy. ^{39}K recoils will be identified event-by-event using a Si telescope (ΔE = 65 μm, $E = 1000$ μm) placed downstream of the target location ($z = 1000$ mm). A 15 mm diameter blocker will be placed in front of the Si telescope to stop un-reacted beam while also allowing for the center-of-mass angular range of the protons noted above. Fig. 3 shows schematically the trajectories for protons and recoils from the lowest and highest excitation energy states of interest.

A simulated excitation energy spectrum for the ^{38}K(d,p) reaction at 7.5 MeV/u is shown in Fig. 4 for all levels with predicted C^2S values > 0.1 and for an expected resolution of 125 keV FWHM. It should be emphasized, that by definition of the MEDs, all states of interest have *known* energies to within $\approx$ 1 keV and so are their spin-parity values which define the ℓ-transfer values. Our goal therefore is **to determine the relative intensities of the peaks in the selective one-neutron adding (d,p) reaction**. In Fig. 4 and Table 1, the relative overlaps (C^2S) for the reaction have been calculated using the successful FSU cross-shell effective interaction [13]. As shown in Fig. 4, only a single state is predicted to carry sizeable strength from $\ell = 1$ transfer below $\sim$6 MeV in

excitation energy ($7/2_4^-$ state at 5.0 MeV). It should be pointed out that though unlikely, if a comparable amount of the $J = 0^+$ isomer were to present in the ^{38}K beam, $\ell = 3$ transfer would occur only to states having $J = 7/2^-$. Therefore, the isomer content would not impact the $J = 9/2^-, 11/2^-$, or $13/2^-$ single-neutron strengths. Furthermore, states populated via transfer on the isomer appear with a known shift in their Q-value by the 130 keV value of the isomer, as in Refs. [19, 20, 21].

Summary of requested shifts: We request **9** shifts of HIE-ISOLDE beam time, 8 of those for data collection and an additional shift for the refinement of the experimental setup and beam tuning. The beam-time estimate is based on the demand for experimental sensitivity ($\approx$ 100 counts) for states with spectroscopic factors down to the 10% level of the expected aligned $13/2^-$ state (see Table 1). The average $\ell = 3$ cross section is around 1.5 mb integrated over the accepted angular range. Combining this information with a total ^{38}K beam rate of 2×10^6 pps, a CD_2 target thickness of 100 μg/cm^2, an experimental acceptance of $\approx$ 60%, and a quenching factor on the single-neutron strengths of 0.6, >2000 counts are expected in the $13/2^-$ state and on the order of 100 counts are expected in the yrast $9/2^-$ and $11/2^-$ levels (Table 1).

References

[1] S. M. Lenzi, N. Mărginean, D. R. Napoli, C. A. Ur, A. P. Zuker, G. de Angelis, A. Algora, M. Axiotis, D. Bazzacco, N. Belcari, M. A. Bentley, P. G. Bizzeti, A. Bizzeti-Sona, F. Brandolini, P. von Brentano, D. Bucurescu, J. A. Cameron, C. Chandler, M. De Poli, A. Dewald, H. Eberth, E. Farnea, A. Gadea, J. Garces-Narro, W. Gelletly, H. Grawe, R. Isocrate, D. T. Joss, C. A. Kalfas, T. Klug, T. Lampman, S. Lunardi, T. Martínez, G. Martínez-Pinedo, R. Menegazzo, J. Nyberg, Zs. Podolyak, A. Poves, R. V. Ribas, C. Rossi Alvarez, B. Rubio, J. Sánchez-Solano, P. Spolaore, T. Steinhardt, O. Thelen, D. Tonev, A. Vitturi, W. von Oertzen, and M. Weiszflog. Coulomb energy differences in $T = 1$ mirror rotational bands in ^{50}fe and ^{50}cr. *Phys. Rev. Lett.*, 87:122501, Aug 2001. URL: https://link.aps.org/doi/10.1103/PhysRevLett.87.122501, doi:10.1103/PhysRevLett.87.122501.

[2] A. P. Zuker, S. M. Lenzi, G. Martínez-Pinedo, and A. Poves. Isobaric multiplet yrast energies and isospin nonconserving forces. *Phys. Rev. Lett.*, 89:142502, Sep 2002. URL: https://link.aps.org/doi/10.1103/PhysRevLett.89.142502, doi:10.1103/PhysRevLett.89.142502.

[3] M.A. Bentley and S.M. Lenzi. Coulomb energy differences between high-spin states in isobaric multiplets. *Progress in Particle and Nuclear Physics*, 59(2):497–561, 2007. URL: https://www.sciencedirect.com/science/article/pii/S0146641006000743, doi:https://doi.org/10.1016/j.ppnp.2006.10.001.

[4] M. A. Bentley, S. M. Lenzi, S. A. Simpson, and C. Aa. Diget. Isospin-breaking interactions studied through mirror energy differences. *Phys. Rev. C*, 92:024310, Aug 2015. URL: https://link.aps.org/doi/10.1103/PhysRevC.92.024310, doi:10.1103/PhysRevC.92.024310.

[5] Michael A Bentley. Excited states in isobaric multiplets – experimental advances and the shell-model approach. *Physics*, 4(3):995–1011, 2022. URL: https://www.mdpi.com/2624-8174/4/3/66, doi:10.3390/physics4030066.

[6] A. Boso, S. M. Lenzi, F. Recchia, J. Bonnard, A. P. Zuker, S. Aydin, M. A. Bentley, B. Cederwall, E. Clement, G. de France, A. Di Nitto, A. Dijon, M. Doncel, F. Ghazi-Moradi, A. Gadea, A. Gottardo, T. Henry, T. Hüyük, G. Jaworski, P. R. John, K. Juhász, I. Kuti, B. Melon, D. Mengoni, C. Michelagnoli, V. Modamio, D. R. Napoli, B. M. Nyakó, J. Nyberg, M. Palacz, J. Timár, and J. J. Valiente-Dobón. Neutron skin effects in mirror energy differences: The case of ^{23}Mg$-^{23}$Na. *Phys. Rev. Lett.*, 121:032502, Jul 2018. URL: https://link.aps.org/doi/10.1103/PhysRevLett.121.032502, doi:10.1103/PhysRevLett.121.032502.

[7] Th. Andersson, D. Rudolph, C. Baktash, J. Eberth, C. Fahlander, D. Haslip, D.R. LaFosse, S.D. Paul, D.G. Sarantites, C.E. Svensson, H.G. Thomas, J.C. Waddington, W. Weintraub, J.N. Wilson, and B.A. Brown. High-spin states in the $a = 39$ mirror nuclei ^{39}ca and ^{39}k. *Eur. Phys. J. A*, 6(1):5–8, 1999. doi:10.1007/s100500050310.

[8] J. Ekman, D. Rudolph, C. Fahlander, A. P. Zuker, M. A. Bentley, S. M. Lenzi, C. Andreoiu, M. Axiotis, G. de Angelis, E. Farnea, A. Gadea, Th. Kröll, N. Mărginean, T. Martinez, M. N. Mineva, C. Rossi-Alvarez, and C. A. Ur. Unusual isospin-breaking and isospin-mixing effects in the $a = 35$ mirror nuclei. *Phys. Rev. Lett.*, 92:132502, Apr 2004. URL: https://link.aps.org/doi/10.1103/PhysRevLett.92.132502, doi:10.1103/PhysRevLett.92.132502.

[9] F. Della Vedova, S. M. Lenzi, M. Ionescu-Bujor, N. Mărginean, M. Axiotis, D. Bazzacco, A. M. Bizzeti-Sona, P. G. Bizzeti, A. Bracco, F. Brandolini, D. Bucurescu, E. Farnea, A. Iordachescu, S. Lunardi, T. Martínez, P. Mason, R. Menegazzo, B. Million, D. R. Napoli, M. Nespolo, P. Pavan, C. Rossi Alvarez, C. A. Ur, R. Venturelli, and A. P. Zuker. Isospin symmetry breaking at high spin in the mirror nuclei ^{35}Ar and ^{35}Cl. *Phys. Rev. C*, 75:034317, Mar 2007. URL: https://link.aps.org/doi/10.1103/PhysRevC.75.034317, doi:10.1103/PhysRevC.75.034317.

[10] D. G. Jenkins, C. J. Lister, M. P. Carpenter, P. Chowdhury, N. J. Hammond, R. V. F. Janssens, T. L. Khoo, T. Lauritsen, D. Seweryniak, T. Davinson, P. J. Woods, A. Jokinen, and H. Penttila. Mirror energy differences in the $a = 31$ mirror nuclei, ^{31}S and ^{31}P, and their significance in electromagnetic spin-orbit splitting. *Phys. Rev. C*, 72:031303, Sep 2005. URL: https://link.aps.org/doi/10.1103/PhysRevC.72.031303, doi:10.1103/PhysRevC.72.031303.

[11] M. Ionescu-Bujor, A. Iordachescu, D. R. Napoli, S. M. Lenzi, N. Mărginean, T. Otsuka, Y. Utsuno, R. V. Ribas, M. Axiotis, D. Bazzacco, A. M. Bizzeti-Sona, P. G. Bizzeti, F. Brandolini, D. Bucurescu, M. A. Cardona, G. de Angelis, M. De Poli, F. Della Vedova, E. Farnea, A. Gadea, D. Hojman, C. A. Kalfas, Th. Kröll, S. Lunardi, T. Martínez, P. Mason, P. Pavan, B. Quintana, C. Rossi Alvarez, C. A. Ur, R. Vlastou, and S. Zilio. High spin structure and intruder configurations in ^{31}P.

Phys. Rev. C, 73:024310, Feb 2006. URL: https://link.aps.org/doi/10.1103/PhysRevC.73.024310, doi:10.1103/PhysRevC.73.024310.

[12] D. A. Testov, A. Boso, S. M. Lenzi, F. Nowacki, F. Recchia, G. de Angelis, D. Bazzacco, G. Colucci, M. Cottini, F. Galtarossa, A. Goasduff, A. Gozzelino, K. Hady, G. Jaworski, P. R. John, S. Lunardi, R. Menegazzo, D. Mengoni, A. Mentana, V. Modamio, A. Nannini, D. R. Napoli, M. Palacz, M. Rocchini, M. Siciliano, and J. J. Valiente-Dobón. High-spin intruder states in the mirror nuclei ^{31}S and ^{31}P. *Phys. Rev. C*, 104:024309, Aug 2021. URL: https://link.aps.org/doi/10.1103/PhysRevC.104.024309, doi:10.1103/PhysRevC.104.024309.

[13] R. S. Lubna, K. Kravvaris, S. L. Tabor, Vandana Tripathi, E. Rubino, and A. Volya. Evolution of the N = 20 and 28 shell gaps and two-particle-two-hole states in the FSU interaction. *Phys. Rev. Research*, 2:043342, Dec 2020. URL: https://link.aps.org/doi/10.1103/PhysRevResearch.2.043342, doi:10.1103/PhysRevResearch.2.043342.

[14] C. R. Hoffman et al. Single-particle aspects of high-j *sd*-shell mirror energy differences (meds). *ATLAS PAC*, 2023. URL: https://www.phy.anl.gov/atlas/pac/exp22May23.html.

[15] D. Tonev, G. de Angelis, I. Deloncle, N. Goutev, G. De Gregorio, P. Pavlov, I.L. Pantaleev, S. Iliev, M.S. Yavahchova, P.G. Bizzeti, A. Demerdjiev, D.T. Dimitrov, E. Farnea, A. Gadea, E. Geleva, C.Y. He, H. Laftchiev, S.M. Lenzi, S. Lunardi, N. Marginean, R. Menegazzo, D.R. Napoli, F. Nowacki, R. Orlandi, H. Penttilä, F. Recchia, E. Sahin, R.P. Singh, M. Stoyanova, C.A. Ur, and H.-F. Wirth. Transition probabilities in 31p and 31s: A test for isospin symmetry. *Phys. Lett. B*, 821:136603, 2021. URL: https://www.sciencedirect.com/science/article/pii/S0370269321005438, doi:https://doi.org/10.1016/j.physletb.2021.136603.

[16] C. M. Perey and F. G. Perey. *Phys. Rev.*, 132:755–773, Oct 1963. URL: https://link.aps.org/doi/10.1103/PhysRev.132.755, doi:10.1103/PhysRev.132.755.

[17] F. G. Perey. *Phys. Rev.*, 131:745–763, Jul 1963. URL: https://link.aps.org/doi/10.1103/PhysRev.131.745, doi:10.1103/PhysRev.131.745.

[18] K. A. Chipps, R. L. Kozub, C. Sumithrarachchi, T. Ginter, T. Baumann, K. Lund, A. Lapierre, A. Villari, F. Montes, S. Jin, K. Schmidt, S. Ayoub, S. D. Pain, and D. Blankstein. *Phys. Rev. Accel. Beams*, 21:121301, Dec 2018. URL: https://link.aps.org/doi/10.1103/PhysRevAccelBeams.21.121301, doi:10.1103/PhysRevAccelBeams.21.121301.

[19] D. Santiago-Gonzalez, K. Auranen, M. L. Avila, A. D. Ayangeakaa, B. B. Back, S. Bottoni, M. P. Carpenter, J. Chen, C. M. Deibel, A. A. Hood, C. R. Hoffman, R. V. F. Janssens, C. L. Jiang, B. P. Kay, S. A. Kuvin, A. Lauer, J. P. Schiffer, J. Sethi, R. Talwar, I. Wiedenhöver, J. Winkelbauer, and S. Zhu. Probing the single-particle character of rotational states in ^{19}F using a short-lived isomeric beam.

Phys. Rev. Lett., 120:122503, Mar 2018. URL: https://link.aps.org/doi/10.1103/PhysRevLett.120.122503, doi:10.1103/PhysRevLett.120.122503.

[20] T. L. Tang, C. R. Hoffman, B. P. Kay, I. A. Tolstukhin, S. Almaraz-Calderon, B. W. Asher, M. L. Avila, Y. Ayyad, K. W. Brown, D. Bazin, J. Chen, K. A. Chipps, P. A. Copp, M. Hall, H. Jayatissa, H. J. Ong, D. Santiago-Gonzalez, D. K. Sharp, J. Song, S. Stolze, G. L. Wilson, and J. Wu. Experimental study of the isomeric state in ^{16}N using the ^{16}N$^{g,m}(d,^3$He) reaction. *Phys. Rev. C*, 105:064307, Jun 2022. URL: https://link.aps.org/doi/10.1103/PhysRevC.105.064307, doi:10.1103/PhysRevC.105.064307.

[21] K. L. Jones, A. Bey, S. Burcher, J. M. Allmond, A. Galindo-Uribarri, D. C. Radford, S. Ahn, A. Ayres, D. W. Bardayan, J. A. Cizewski, R. F. Garcia Ruiz, M. E. Howard, R. L. Kozub, J. F. Liang, B. Manning, M. Matos, C. D. Nesaraja, P. D. O'Malley, E. Padilla-Rodal, S. D. Pain, S. T. Pittman, A. Ratkiewicz, K. T. Schmitt, M. S. Smith, D. W. Stracener, and R. L. Varner. *Phys. Rev. C*, 105:024602, Feb 2022. URL: https://link.aps.org/doi/10.1103/PhysRevC.105.024602, doi:10.1103/PhysRevC.105.024602.

DESCRIPTION OF THE PROPOSED EXPERIMENT

The experimental setup comprises: ISOLDE solenoidal spectrometer

Part of the	Availability	Design and manufacturing
ISS	☒ Existing	☒ To be used without any modification ☐ To be modified
	☐ New	☐ Standard equipment supplied by a manufacturer ☐ CERN/collaboration responsible for the design and/or manufacturing

HAZARDS GENERATED BY THE EXPERIMENT (if using fixed installation:) Hazards named in the document relevant for the fixed [MINIBALL + only CD, MINIBALL + T-REX] installation.

Additional hazards:

Hazards			
Thermodynamic and fluidic			
Pressure			
Vacuum			
Temperature	4 K		

Heat transfer			
Thermal properties of materials			
Cryogenic fluid	LHe, ∼1650 l, LN_2, ∼200 l, 1.0 Bar		
Electrical and electromagnetic			
Electricity	0 V, 300 A		
Static electricity			
Magnetic field	2.5 T		
Batteries			
Capacitors			
Ionizing radiation			
Target material	Deuterated polyethylene		
Beam particle type	^{38}K		
Beam intensity	2×10^6 pps		
Beam energy	7.5 MeV/u		
Cooling liquids			
Gases			
Calibration sources:	☒		
• Open source	☒ (α calibration sources)		
• Sealed source			
• Isotope			
• Activity			
Use of activated material:			
• Description			
• Dose rate on contact and in 10 cm distance			
• Isotope			
• Activity			
Non-ionizing radiation			
Laser			
UV light			
Microwaves (300MHz-30 GHz)			

Radiofrequency (1-300 MHz)			
Chemical			
Toxic			
Harmful			
CMR (carcinogens, mutagens and substances toxic to reproduction)			
Corrosive			
Irritant			
Flammable			
Oxidizing			
Explosiveness			
Asphyxiant	Helium		
Dangerous for the environment			
Mechanical			
Physical impact or mechanical energy (moving parts)			
Mechanical properties (Sharp, rough, slippery)			
Vibration			
Vehicles and Means of Transport			
Noise			
Frequency			
Intensity			
Physical			
Confined spaces			
High workplaces			
Access to high workplaces			
Obstructions in passageways			
Manual handling			
Poor ergonomics			

Hazard identification:

Average electrical power requirements (excluding fixed ISOLDE-installation mentioned above): N/A